

## Measurements and reinterpretation of spin splitting in antimony using the de Haas-van Alphen effect

P. H. Hill and J. Vanderkooy

*Department of Physics, University of Waterloo, Waterloo, Ontario, Canada N2L 3G1*

(Received 13 August 1976; revised manuscript received 6 October 1977)

By using the de Haas-van Alphen (dHvA) effect,  $g$  factors have been determined in antimony for most carrier branches in the trigonal-bisectrix and binary-bisectrix planes. The use of magnetic fields to 11.8 T, low-level field modulation, and annealed samples allowed accurate determination of the relative spin splitting by direct observation of the dHvA wave shape. Infinite-field phase extrapolations show that  $g$  factors are much lower than previously reported. This is shown to be in agreement with theoretical expectations for these  $g$  factors.

### INTRODUCTION

Antimony has been studied by many investigators, and specific experiments have been done relating to the effects of spin on the electronic energy levels near the Fermi surface.<sup>1,2</sup> In such experiments the assignment of the spin splitting has been prejudiced by the belief that the carriers in antimony should act similarly to the electrons in bismuth.<sup>3</sup> Direct observation of spin splitting was seen in the magnetothermal oscillations of antimony,<sup>4</sup> but no definite level assignment was given. A dHvA study of antimony<sup>5</sup> observed a number of spin zeroes which give accurate orientations for which the spin splitting is half the Landau-level separation.

The  $g$  values from spin-splitting dHvA studies in a recent paper<sup>6</sup> did not agree with our own data based on direct observation of the effects of spin on the dHvA wave shape. The present paper reports on a systematic study of antimony to obtain more accurate and complete data. Our measurements have led us to question the validity of the condition  $g \sim 2m_0/m$  for antimony. Results indicate that the spin-splitting is usually small and becomes equal to or slightly larger than half the Landau-level separation only in a small angular range as defined by the spin zeroes of Windmiller.<sup>5</sup>

### EXPERIMENTAL

The detection of the de Haas-van Alphen (dHvA) oscillations was first begun using a torque magnetometer.<sup>7</sup> However, experimental difficulties together with the low harmonic content of the oscillations prompted a change to the field-modulation method.

The experimental setup followed conventional lines.<sup>8</sup> The magnet was a superconducting solenoid capable of fields to 11.8 T. Field determination was by a magnetoresistance probe which had

been NMR calibrated to within 0.1%. The modulation frequency was 220 Hz which permitted full penetration of the modulation field into the sample due to the high magnetoresistance of antimony. The use of low-level modulation (approximately 0.0015 T peak to peak) ensured the absence of any smearing of the wave shape at high fields. All detection was done at the fundamental of the modulation frequency and the sample temperature was approximately 1.3 K.

Samples were spark cut into approximately 25-mm<sup>3</sup> cubes and annealed in helium. At first the sample was glued to a sheet of phosphor bronze with varnish and the assembly was spring mounted in the sample holder. This method always gave dHvA oscillations with a high Dingle temperature, especially after thermal cycling to room temperature. It was noted that the Dingle temperature was roughly proportional to the number of thermal cycles between liquid helium and room temperatures, indicating probably a dislocation density proportional to the total number of thermal cycles. The second method of mounting the sample was similar to the first, but no varnish was used, and the Dingle temperature stayed low even after several intermediate cycles to room temperatures.

### THEORETICAL PREDICTIONS FOR WAVE SHAPE AND INFINITE-FIELD PHASE

For detection of the dHvA effect by low-level, low-frequency modulation at the modulation frequency the signal  $V$  is given by the proportionality<sup>9</sup>

$$V \propto \frac{1}{B^{5/2}} \sum_{r=1}^{\infty} r^{1/2} \frac{\exp(-r\lambda X/B)}{\sinh(r\lambda T/B)} \times \cos\left(\frac{2\pi r F}{B} - 2\pi r \gamma \pm \frac{\pi}{4}\right) \cos\left(\frac{r\pi g m}{2m_0}\right) \quad (1)$$

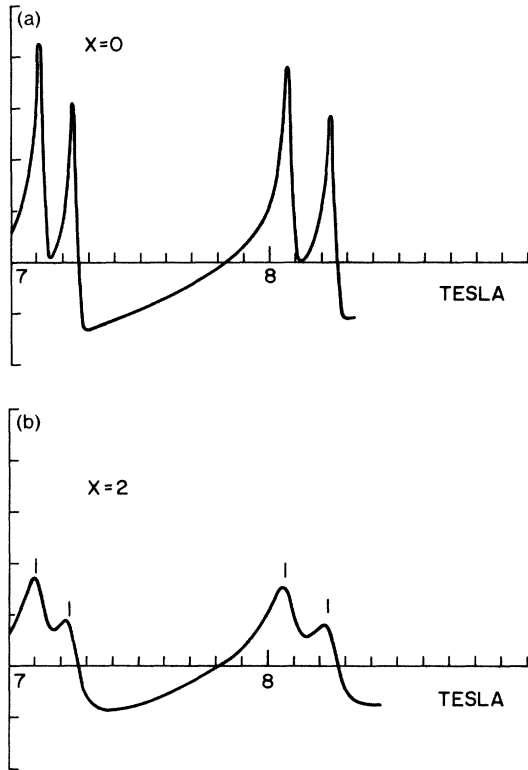


FIG. 1. Calculated wave forms for first harmonic detection including 30 harmonics showing the effect of the Dingle temperature on the spin-split wave form. In both cases  $T = 1.3$  K,  $m_c = 0.06$ ,  $g = 5$ , and  $F = 60$  T. (a)  $X = 0$ ; (b)  $X = 2$  K. The marks indicate peak positions for  $X = 0$ .

where  $\lambda = 2\pi^2 km / e\hbar$ ,  $X$  is the Dingle temperature,  $m$  is the cyclotron mass,  $m_0$  is the free-electron mass, and the other symbols have their usual meaning. The last cosine factor is often written as  $\cos(\gamma\pi S)$ . For antimony the Fermi surface has a maximum extremal area, so  $-\frac{1}{4}\pi$  must be used, and we expect  $\gamma = \frac{1}{2}$  as for free electrons. Figure 1 shows examples of wave shapes computed from (1) which are relevant to the antimony problem. Fig. 1(a) shows the expected wave shape at high field  $B \approx 8T$ ,  $T = 1.3$  K,  $m = 0.06m_0$ ,  $g = 5$ , and the Dingle temperature  $X = 0$  while Fig. 1(b) assumes  $X = 2$  K. Similar calculations for lower values of  $B$  show that spin splitting is not observable below 5 T for  $X$  as high as 2 K. This clearly demonstrates the importance of having a good sample, i.e., a low Dingle temperature, if direct observation of spin splitting is to be used for determining  $g$  factors.

Good examples of observed experimental wave shapes can be seen for low fields in Fig. 2(a), and high fields in Fig. 2(b). The latter shows

clearly the asymmetry seen in the computed wave shape of Fig. 1(a). The sharp peaks allow a determination of the magnetic field at which a Landau level passes through the Fermi surface. It is clear from the observations of Fig. 2(b) that the peaks point upwards, and the smooth parts of the oscillations are at the bottom as in Fig. 1. The complexity of the observations is due to the existence of at least two sets of spin-split peaks, each with its own dHvA frequency  $F$ . Fig. 2(c) shows data taken at the same orientation as Fig. 2(b), but the Dingle temperature was much higher due to thermal stresses from the sample mounting. It is far more difficult to differentiate peaks from the smooth bottoms of the oscillations because of the reduced dHvA harmonic content.

In the interpretation of the experiments we shall not make any detailed use of the dHvA wave shape as given by (1), but use only the fact that the position of a cusp or sharp peak corresponds closely to the passage of a Landau level through the Fermi surface extremal area. It is possible that the peak positions could be slightly shifted due to fluctuations of the Fermi energy, but the analysis presented later does not show any significant anomalies.

The extraction of  $g$  factors and relative spin splitting from observed oscillations such as those of Fig. 2 is not unique. This is illustrated by the momentum space area quantization scheme shown in Fig. 3, which can also be regarded as an energy level scheme if we restrict the Landau-level separation to be constant away from the Fermi surface. It can be seen that a given observed pattern of oscillation peaks (caused by the sweep of magnetic field which increases areas and sweeps the levels through the Fermi surface area) is compatible with a whole series of level schemes. These fall into two distinct categories, which we shall call type *A* and type *B*. For type *A*, the effects of spin are such that the levels before consideration of spin fall between closely spaced pairs of levels. In type-*B* splitting, the levels before spin are considered to lie between the larger final level spacings.

The cusps of the oscillations come at fields  $B_n$  such that

$$F/B_n = n + \frac{1}{2} \pm \frac{1}{2}(p \pm S_0), \quad (2)$$

where  $p$  is an integer,  $S_0$  is defined to lie between 0 and  $\frac{1}{2}$  (and has the significance indicated in Fig. 3), and the true spin splitting  $S$  which enters into Eq. (1) is

$$S = p \pm S_0, \quad (3)$$

in which the  $\pm$  takes into account the ambiguity as to which way the spin effects can occur even

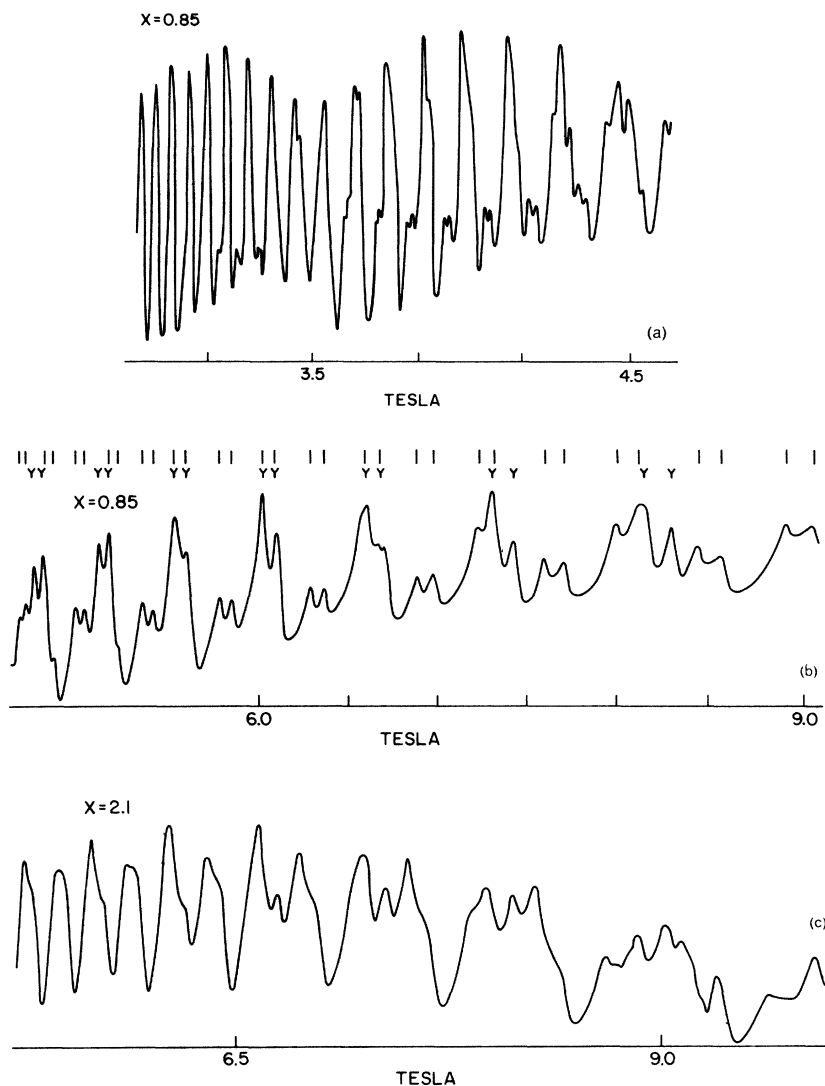


FIG. 2. Experimentally observed wave forms for first harmonic detection. (a) Low-field region showing one dominant frequency and the development of a second frequency at higher field. The crystal is oriented at  $24.5^\circ$  from the trigonal towards  $\Gamma X$  in the trigonal-bisectrix plane; (b) High field region of (a) indicating the wave shape with spin-splitting observable. The two lowest mass carriers are observable with the electrons indicated as 1's and the holes as Y's; (c) Trace showing the effect of high Dingle temperature. Two frequencies are present but splitting is not observable until approximately 7 T.

though  $S_0$  is defined to be positive. The additional  $\pm$  in Eq. (2) takes into account the two spin directions. Even values of  $p$  are type-A splitting and the cases  $p=0(\pm)$  and  $p=2(-)$  are illustrated in Fig. 3. Type-B splitting corresponds to odd values of  $p$  and the cases  $p=1(-)$  and  $p=1(+)$  are also illustrated in Fig. 3.

In principle spin resonance data should resolve the ambiguities as to which is the true value of  $S$ , but unfortunately the experimental evidence<sup>1,2</sup> is complicated and difficult to interpret reliably. However it is possible to restrict the ambiguity<sup>10</sup>

to a great extent by examining the dHvA phase of the cusps at high magnitude fields and to determine whether  $p$  is odd or even. This can be done by subtracting from the  $F/B_n$  values of a pair of neighboring cusps the largest integer which will reduce the values to positive fractions which differ by less than  $\frac{1}{2}$ . If  $p$  is even, the mean of these two fractions should be  $\frac{1}{2}$ , while if  $p$  is odd, the mean should be 1. The actual value of  $p$  and the sign to be used with  $S_0$  in Eq. (3) cannot of course be determined in this way. Illustrations of this procedure will be presented in the next section.

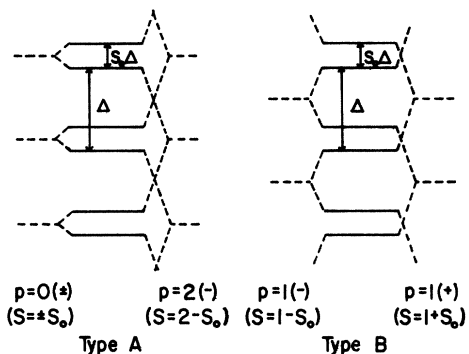


FIG. 3. Diagram illustrating momentum space area quantization schemes including the effects of spin. Two schemes, types A and B, are shown. The dotted lines illustrate the original Landau levels without spin and the association to the solid lines is drawn to indicate the effects of spin. The notation  $p$  with the spin refers to Eq. (2) and (3) of the text.  $S_0$  is the positive fractional splitting between Landau levels separated by a momentum space area  $\Delta$ . Our work shows that the first choice  $p = 0(\pm)$  is the correct one.

EXPERIMENTAL RESULTS

Examples of observed oscillation traces are shown in Figs. 2 and 4. In Fig. 2 only two superimposed dHvA frequencies are present, each spin-split, and in Fig. 4 there are probably four superimposed frequencies, each of which has spin-split peaks. The harmonic content of the oscillations increases with field until they become clearly recognizable peaks, of the cusplike nature predicted by the theory. From knowledge of the accurate  $F$  values deduced from the low field data (which agree with the values of Windmiller<sup>5</sup>) it is possible to identify the pairs of peaks which be-

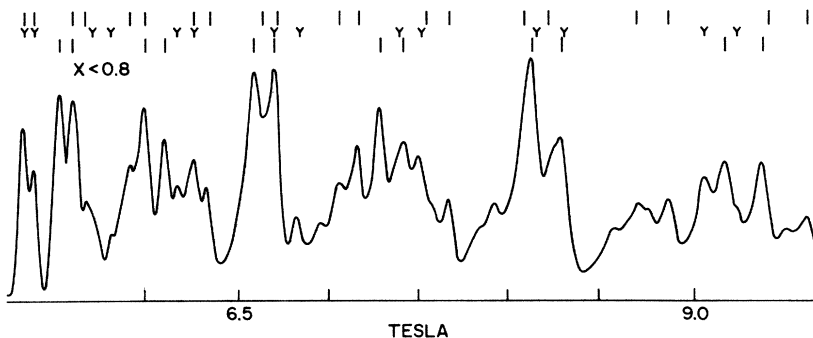


FIG. 4. Experimentally observed wave form showing high harmonic content and the large number of identifiable oscillations. The crystal was oriented at approximately  $23^\circ$  from the binary in the binary-bisectrix plane. The electrons are identified by I's and the holes by Y's. The most easily identified frequencies are shown toward the bottom and the hardest at the top. The top row of labels should be regarded as tentative. The frequencies are 69.4, 77.5, and 108.7 T from bottom to top, respectively. At high fields more peaks emerge that are not easily analyzed.

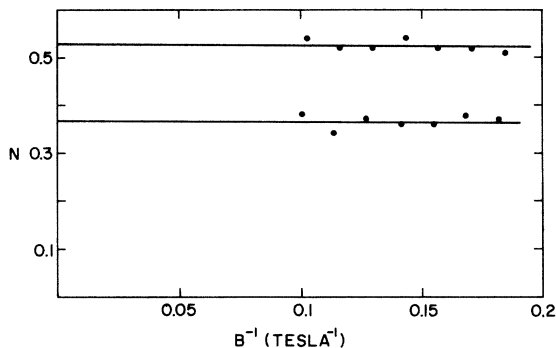


FIG. 5. Plot of reduced quantum number ( $N$ ) for the light electrons in the binary-bisectrix plane at  $7^\circ$  from the binary showing the infinite-field intercept.

long to each separate frequency, as indicated by the labelling of the experimental traces.

The procedure of the previous section using  $F/B_n$  values for examining the high field phase is illustrated by the plots of Figs. 5 and 6 for electrons and holes, respectively, at one particular orientation. It can be seen that the "reduced" phase thus obtained lies close to  $\frac{1}{2}$ , indicating that  $p$  is even for both electrons and holes. A small error in  $F$  is probably responsible for the slope of these curves, while slight errors in using the peaks to estimate where the Landau level has crossed the Fermi surface could prevent the plots from being centered exactly on  $\frac{1}{2}$ .

The result that  $p$  is even was found for all the orientations studied, so that the true splitting is given by

$$S = S_0 \text{ or } 2 \pm S_0 \text{ or } 4 \pm S_0, \text{ etc.}$$

The most plausible assignment for reasons to be

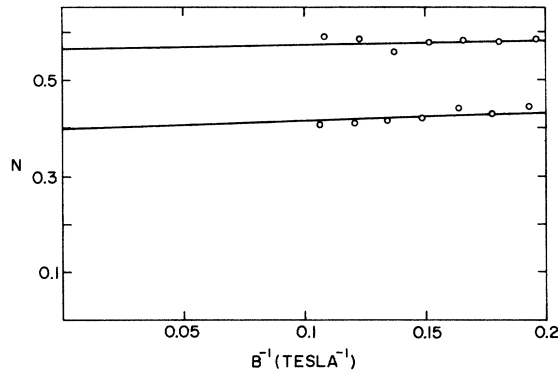


FIG. 6. Reduced quantum number plot for the holes showing the infinite-field intercept.

discussed in the next section is  $S=S_0$ , and plots of  $S_0$  at different orientations are presented in Figs. 7 and 8. Values of  $g$  can be obtained from the relation

$$S = \frac{1}{2} g m_c / m_0$$

and are plotted in Figs. 9 and 10, but these are appreciably less accurate than the  $S$  values because the masses  $m_c$  are known only to an accuracy of order 10%.<sup>11</sup> In contrast, the  $S$  values of relative splitting can be determined to 1%. The dHvA effect really measures  $S$  (or  $S_0$ ), and not the  $g$  value, so that it would be more consistent to give results in terms of plots such as Figs. 7 and 8.

#### DISCUSSION

Our choice of  $p=0$  in Eq. (3) as outlined in the previous sections gives  $g$  values which differ from those reported elsewhere.<sup>2,6</sup> The range of  $g$  values obtained is in agreement with that predicted by

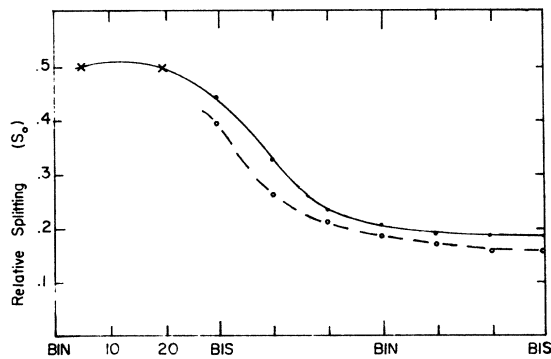


FIG. 7. Relative splitting values ( $S_0$ ) in the binary-bisectrix plane. The solid line indicates hole and the dashed line electron values of  $S_0$ . X's indicate Windmill spin zeroes. Heavy cyclotron mass values are to the left and light masses to the right. Only one of three sets of curves is shown for clarity.

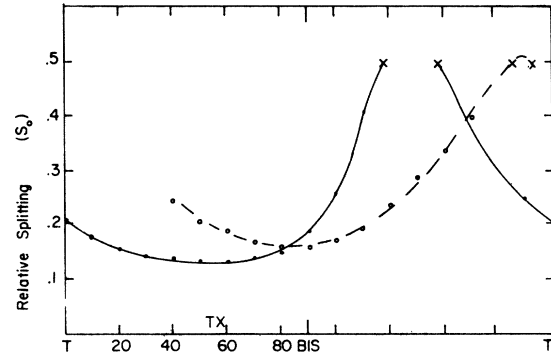


FIG. 8. Relative splitting values ( $S_0$ ) in the trigonal-bisectrix plane. X's indicate Windmill spin zeroes. Only principal hole and electron carriers are shown.

Dupree and Holland.<sup>12</sup> They give the upper limit to a shift of the  $g$  value from that of free electrons as

$$|\Delta g| \leq 4l_j^2 \Delta_j / (2l_j + 1) \delta_j(k) \quad (4)$$

where  $\Delta_j$  is the largest spin-orbit coupling constant for atomic orbitals contributing to the Fermi wave functions;  $l_j$  is the corresponding azimuthal quantum number and  $\delta_j(k)$  is the band gap to the nearest state of appropriate symmetry. Randles<sup>13</sup> points out that this upper value does not include many-body effects, but such effects are not expected to be significant in relation to spin-orbit effects which are very important in this study. For antimony,  $\Delta_j$  is 0.49 eV,<sup>6</sup>  $l_j=1$  corresponding to the  $p$  level, and  $\delta_j(k)=0.1$  eV.<sup>14</sup> Then we have  $|\Delta g| < 6.5$ .

This upper limit for the  $g$ -factor shift in antimony is in agreement with experimental values only using  $p=0$  in Eq. (3). For antimony odd values of  $p$  are excluded by the infinite field phase measurements whereas  $p \geq 2$  leads to  $g$  factors

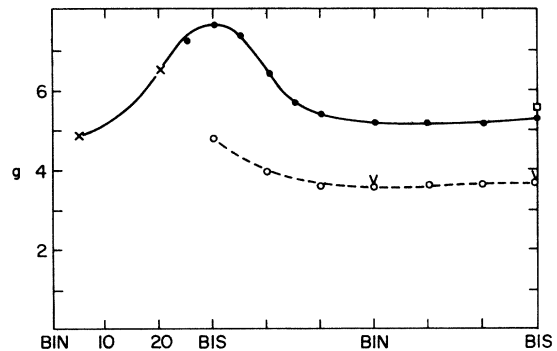


FIG. 9.  $g$ -factor values in the binary-bisectrix plane. The solid line indicates hole, and the dashed line electron  $g$ -factor values. X's indicate Windmill (Ref. 7) spin-split zeroes; V's indicate electron and  $\square$ 's hole  $g$ -factor values obtained by McCombe and Seidel (Ref. 6).

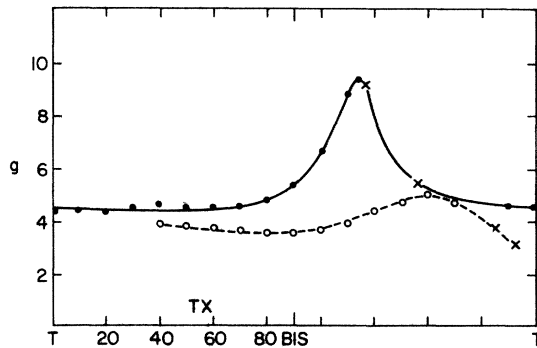


FIG. 10.  $g$ -factor values in the trigonal-bisectrix plane. The solid line indicates holes, and the dashed line electron  $g$ -factor values. X's indicate Wmdmiller (Ref. 7) spin-split zeroes.

which are in excess of that predicted by Cohen and Blount. Thus  $p=0$  is the only choice remaining. The choice of  $p=1$  (and a sign such that  $S=1-S_0$ ) in previous investigations<sup>1,2,6</sup> of antimony is probably due to the belief that antimony should be comparable to bismuth in its behavior. However, the band gap in bismuth is almost an order of magnitude smaller,  $\delta_j=0.013$  eV,<sup>15</sup> and the spin-orbit coupling is much larger,  $\Delta_j=1.86$  eV,<sup>16</sup> which from Eq. (4) indicates that  $|\Delta g| \leq 200$ . This value for bismuth is in reasonable agreement with the experimental value of up to 225. Cohen and Blount<sup>3</sup> have shown that for the large spin-orbit coupling in bismuth, one expects

$$g \sim 2m_0/m \quad (5)$$

in agreement with experiments for the electrons. This implies a level separation due to spin equal to the Landau-level separation. Hence for bismuth  $p=1$  with  $S_0=0$ , but our experiments show this cannot be valid for antimony. In general, we may consider that as a function of increasing spin-orbit coupling, the  $g$  factor is proportional to spin orbit coupling  $\Delta_j$  at low values but limited by Eq. (4), and as the coupling increases the  $g$  factor is given by Eq. (5). The spin-orbit coupling and band gap for antimony indicate (4) is applicable, while the larger spin-orbit coupling and much smaller band gap show that (5) is applicable for the electrons in bismuth.

The peak of the  $g$  factor curve for the holes in Fig. 10 is noticeably different from the minimum of the mass curve in the cyclotron resonance work.<sup>11</sup> For the electrons this is somewhat less true. In any event Eq. (5) has thus little bearing on the  $g$  factors. The deviations may be due to the nonellipsoidal nature of the Fermi surface pockets which are more pronounced for the hole pockets than the electron pockets.<sup>17</sup>

#### COMPARISON WITH EARLIER WORK

In their determination of  $g$  factors from magnetothermal oscillations for the light electrons in the binary-bisectrix plane and for the light hole along the bisectrix axis, McCombe and Seidel<sup>4</sup> list three possible  $g$  values. Agreement with our data at these points is better than 5% if the small splitting is chosen ( $S=\pm S_0$ ) and better than 1% if a larger ( $S=1-S_0$ ) but incorrect splitting is chosen. The larger discrepancy for the first choice is simply due to the larger percentage error because the associated levels are close together.

The  $g$  factor values of antimony in the ESR work of Datars<sup>2</sup> were based on a level assignment of Smith, Galt, and Merritt,<sup>3</sup> which in turn was based on the observed splitting in bismuth. There is, however, no experimental evidence that this association is correct. The change of level assignment that we propose makes no changes in the position of observed resonances but it changes the labelling of spin, cyclotron, and combined resonances. The type-4 resonance<sup>2</sup> is not allowed, but none of the data is incompatible with the new scheme.<sup>18</sup>

Recently Altounian and Datars<sup>6</sup> have obtained  $g$ -factor values in antimony for the lower mass carriers in both the trigonal-bisectrix and trigonal-binary planes. The  $g$  factors were obtained from the harmonic content of the oscillations following the method described by Randles.<sup>13</sup> The choice of splitting was determined from the infinite field phase intercept of dHvA fundamental oscillations. However, the deductions from their intercept of  $-0.56$  for electrons and  $-0.58$  for holes are in disagreement with our calculations. These intercepts imply negative spin factors for the fundamental according to their Eqs. (7) and (8). We believe the sign of the spin factor is incorrectly specified by (7) and (8) in their paper,<sup>6</sup> and that the assignment should be reversed. Equation (7) refers to the magnetization, where the expected variation for the fundamental is  $-\sin 2\pi(F/B - \gamma - \frac{1}{8} - \frac{1}{4} \pm \frac{1}{4})$ , the  $\pm$  sign referring to positive and negative spin factors, respectively. Positive maxima of this term occur when the total phase in the bracket is  $N - \frac{1}{4}$ , where  $N$  is an integer. If we impose the same convention on the infinite phase as Coleridge and Templeton,<sup>19</sup> then the infinite field phase turns out to be  $\phi_0 = -\gamma - \frac{1}{8} - \frac{1}{4} \pm \frac{1}{4}$  which for antimony gives  $-\frac{5}{8}$  and  $-\frac{3}{8}$  for positive and negative spin factor, respectively, precisely the reverse of the conclusion of Altounian and Datars.<sup>6</sup>

Our own procedure for the infinite-field intercept used the shape of the oscillations at high magnetic fields to determine their sense. In con-

trast, dHvA experiments having only a low harmonic content may have uncertainty in the sign of the signal from the pickup coil. This simplicity of our analysis makes us confident in our interpretation. In order to make a valid numerical comparison with the results of Altounian and Datars,<sup>6</sup> we have analyzed our data using the now erroneous relation  $S = 1 - S_0$ . Our  $g$ -factor values then differed by up to 25% from their values in the lowest mass directions. These differences have not as yet been explained. It is, however, in these directions that the spin splitting is most easily observed in the present work because the oscillations are strong and easily analyzed.

#### CONCLUSION

We have shown that high magnetic fields, low-level modulation, and annealed samples allow

accurate deductions to be made about spin splittings in antimony. The results show that antimony is not close to the Cohen and Blount conditions in bismuth where  $g \sim 2m_0/m$ . Experiments that depend on the assignment of Landau level numbers or spin such as magnetoreflexion<sup>14</sup> should be re-evaluated in the light of these results.

#### ACKNOWLEDGMENTS

We thank Dr. W. R. Datars and Dr. Z. Altounian for some useful discussions about their experiments. Dr. D. Shoenberg has made several valuable suggestions, in particular relating to the presentation of the infinite field intercept. We are grateful to the National Research Council of Canada for support of this research.

<sup>1</sup>G. E. Smith, J. K. Galt, and F. R. Merritt, *Phys. Rev. Lett.* **4**, 276 (1960).

<sup>2</sup>W. R. Datars, *Phys. Rev.* **126**, 975 (1962).

<sup>3</sup>M. H. Cohen and E. I. Blount, *Philos. Mag.* **5**, 115 (1960).

<sup>4</sup>B. McCombe and G. Seidel, *Phys. Rev.* **155**, 633 (1967).

<sup>5</sup>L. R. Windmiller, *Phys. Rev.* **149**, 472 (1966).

<sup>6</sup>Z. Altounian and W. R. Datars, *J. Phys. F* **6**, 1297 (1976).

<sup>7</sup>J. Vanderkooy, *J. Phys. E* **2**, 718 (1969).

<sup>8</sup>D. Shoenberg and P. J. Stiles, *Proc. R. Soc. A* **281**, 62 (1964).

<sup>9</sup>A. Goldstein, S. J. Williamson, and S. Foner, *Rev. Sci. Instrum.* **36**, 1356 (1965).

<sup>10</sup>I. M. Templeton, *Phys. Rev. B* **5**, 3819 (1972).

<sup>11</sup>W. R. Datars and J. Vanderkooy, *IBM J. Res. Dev.* **8**, 247 (1964). (The assignments of holes and elec-

trons should be reversed.)

<sup>12</sup>R. Dupree and B. W. Holland, *Phys. Status Solidi* **24**, 275 (1967).

<sup>13</sup>D. L. Randles, *Proc. R. Soc. A* **331**, 85 (1973).

<sup>14</sup>M. S. Dresselhaus and J. G. Mavroides, *Phys. Rev. Lett.* **14**, 259 (1965).

<sup>15</sup>U. Strom, Avid Kamgar, and J. F. Koch, *Phys. Rev. B* **7**, 2435 (1973).

<sup>16</sup>E. U. Condon and G. H. Shortley, *The Theory of Atomic Spectra* (Cambridge U. P., Cambridge, 1935), p. 179.

<sup>17</sup>L. M. Falicov and P. J. Lin, *Phys. Rev.* **141**, 562 (1966).

<sup>18</sup>W. R. Datars (private communication).

<sup>19</sup>P. T. Coleridge and I. M. Templeton, *J. Phys. F* **2**, 643 (1972).